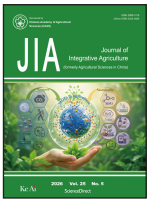
Journal of Integrative Agriculture 2026, 25(5): 1822–1835

KeAi
CHINESE ROOTS
GLOBAL IMPACT

Available online at ScienceDirect

Journal of Integrative Agriculture



RESEARCH ARTICLE

QTL mapping of maize plant height based on a population of doubled haploid lines using UAV LiDAR high-throughput phenotyping data

Xin Zhang[1, 2, 3, 4*], Jidong Zhang[5*], Yunling Peng[1], Xun Yu[3, 4], Lirong Lu[3, 4], Yadong Liu[3, 4], Yang Song[3, 4], Dameng Yin[3, 4], Shaogeng Zhao[2], Hongwu Wang[5#], Xiuliang Jin[3, 4#], Jun Zheng[1, 2#]

[1] *Agronomy College, Gansu Agricultural University, Lanzhou 730070, China*
[2] *State Key Laboratory of Crop Gene Resources and Breeding/Institute of Crop Sciences, Chinese Academy of Agricultural Sciences, Beijing 100081, China*
[3] *State Key Laboratory of Crop Physiology and Ecology, Institute of Crop Sciences, Chinese Academy of Agricultural Sciences, Beijing 100081, China*
[4] *National Nanfan Research Institute (Sanya), Chinese Academy of Agricultural Sciences, Sanya 572000, China*
[5] *National Engineering Research Center of Crop Molecular Breeding/Institute of Crop Sciences, Chinese Academy of Agricultural Sciences, Beijing 100081, China*

Highlights

- Unmanned aerial vehicle (UAV) light detection and ranging (LiDAR) was used for high throughput maize plant height phenotyping in 270 doubled haploid (DH) lines across multiple stages and environments.
- Single plant scale estimation outperformed row scale, with R^2 values of 0.67 *vs*. 0.56 and RMSE values of 0.12 m *vs*. 0.17 m, respectively.
- Using inclusive composite interval mapping, we identified 12 and 20 QTLs for plant height in two DH populations. These results support the feasibility of UAV-based QTL mapping and candidate gene discovery in maize.

Abstract

Maize (*Zea mays* L.) is a globally significant crop that plays a crucial role in feeding the world's growing population. Among its various traits, plant height is particularly important as it affects yield, lodging resistance, ecological adaptability, and other important factors. Traditional methods for measuring plant height often lack cost-efficiency and accuracy. In this study, a light detection and ranging (LiDAR) sensor mounted on an unmanned aerial vehicle (UAV) was employed to collect point cloud data from 270 doubled haploid (DH) lines. This innovative application of UAV-based LiDAR technology was explored for high-throughput phenotyping in maize breeding trials. High-density genetic maps were constructed, and plant height was assessed at both single-plant and row scales across multiple developmental stages and genetic backgrounds. The findings revealed that for many varieties and small areas, single-plant-scale estimation accuracy was superior to row-scale estimation, with R^2 values of 0.67 *vs*. 0.56 and RMSE values of 0.12 m *vs*. 0.17 m, respectively. Two high-density genetic maps were constructed based on SNP markers. In Sanya and Xinxiang, the F_1DH and F_2DH populations identified 12 and 20 QTLs (quantitative trait loci) for plant height, respectively. This study successfully identified and validated QTLs associated with plant height, thereby revealing novel genetic loci and candidate genes. This research highlights the potential of UAV-based remote sensing to advance precision agriculture by enabling efficient, large-scale phenotyping and gene discovery in maize breeding programs.

Keywords: doubled haploid, light detection and ranging, quantitative trait loci, high-density genetic map, unmanned aerial vehicle

Received 12 April 2024; Received in revised form 5 July 2024; Accepted 4 August 2024; Available online 11 September 2024
[#]Correspondence Jun Zheng, E-mail: zhengjun02@caas.cn; Xiuliang Jin, E-mail: jinxiuliang@caas.cn; Hongwu Wang, E-mail: wanghongwu@caas.cn
[*] These authors contributed equally to this study.

© 2026 CAAS. Publishing services by Elsevier B.V. on behalf of KeAi Communications Co. Ltd. This is an open access article under the CC BY-NC-ND license (http://creativecommons.org/licenses/by-nc-nd/4.0/). Peer review under responsibility of Editorial Board of *Journal of Integrative Agriculture*.
doi: 10.1016/j.jia.2024.09.004

1. Introduction

Maize (*Zea mays* L.) is a crucial food crop that supplies at least 30% of the caloric intake for billions of people in many developing countries. Its significance also extends to national economies and social development. With the global population growing and economic development advancing, the urgency of increasing maize yields to ensure food security has intensified (Chardon *et al.* 2004; Heerwaarden *et al.* 2011; Shiferaw *et al.* 2013). A key factor in achieving higher yields is plant height, a crucial breeding trait closely associated with maize productivity (Guo F *et al.* 2021; Yu *et al.* 2022). Developing varieties with optimal plant height is essential for achieving high and stable maize yields (Veldboom and Lee 1996; Teng *et al.* 2013). A comprehensive understanding and optimization of this quantitative trait can enable the development of cultivars that are better adapted to diverse environments, ultimately leading to higher yields to meet the growing global food demand.

Maize plant height is influenced by both genetic and environmental factors. The field of genomic research is rapidly expanding due to advancements in sequencing technology (Liu M *et al.* 2021; Xie *et al.* 2021; Yang L *et al.* 2021; Kumar *et al.* 2022). Researchers have identified numerous genetic loci associated with plant height through quantitative trait loci (QTLs) mapping and genome-wide association studies (GWAS) by leveraging field measurements of plant height. In addition, QTL fine mapping and mutant-based studies have enabled the cloning of key genes that regulate plant height (Radanović *et al.* 2015; Zhou *et al.* 2016, 2018; Du *et al.* 2021; Wang *et al.* 2023). Despite these advances, genetic analysis still relies heavily on phenotyping data. However, traditional methods of phenotyping in the field are labor-intensive and time-consuming (Han *et al.* 2018; Malambo *et al.* 2018; Fei *et al.* 2023). Furthermore, the subjective nature of selecting representative plants during phenotyping compromises accuracy, which poses a bottleneck for genetic research and breeding (Shi *et al.* 2016; Yang W *et al.* 2021; Diepenbrock *et al.* 2022).

Fortunately, the challenge of phenotyping data collection has been addressed with the development of advanced indoor high-throughput phenotyping platforms. These platforms enable the measurement of traditional agronomic traits, and the results are systematically monitored and analyzed (Yang *et al.* 2014; Zhang *et al.* 2017). These automated and high-throughput systems reduce time and increase accuracy in phenotyping, which facilitates the identification of known genes and novel loci in maize, and thus enhances gene discovery capabilities (Wang X *et al.* 2019; Wang *et al.* 2023). However, these indoor platforms are impractical for large-scale breeding trials due to their immobility, prohibitive costs, and limited real-time monitoring capabilities. In contrast, unmanned aerial vehicle (UAV)-based high-throughput phenotyping platforms offer flexibility, precision, and efficiency in data acquisition at a lower cost (Hu *et al.* 2018; Cui *et al.* 2021; Lu *et al.* 2022; Rodene *et al.* 2022). Advanced sensor technologies such as optical, hyperspectral, and light detection and ranging (LiDAR) sensors enable the efficient acquisition of diverse data (Yang W *et al.* 2020; Jin *et al.* 2021; Liu S *et al.* 2021; Araus *et al.* 2022; Bai *et al.* 2022; Cheng *et al.* 2022), thereby facilitating genetic studies (Duan *et al.* 2016; Jiang *et al.* 2021). Currently, some methods for estimating plant height using UAV phenotyping platforms have been developed (Malambo *et al.* 2018; Che *et al.* 2020; Zhou *et al.* 2020; Gilliot *et al.* 2021; Guo Y *et al.* 2021; Luo *et al.* 2021; Shu *et al.* 2022). UAV remote sensing is primarily used to estimate plant height by calculating the difference between the Digital Surface Model (DSM) and the Digital Terrain Model (DTM) (Watanabe *et al.* 2017; Pugh *et al.* 2018; Yu D *et al.* 2020; Lu *et al.* 2021). Some studies that measured plant height at multiple time points using UAV remote sensing for sorghum have shown that UAV-based high-throughput phenotyping outperformed traditional field phenotyping in terms of observation frequency (Pugh *et al.* 2018). However, the variables recorded by researchers varied across different studies, and the optimal statistical variables for estimating plant height differed among these studies (Luo *et al.* 2021; Shu *et al.* 2022).

For genetic analysis, a high-resolution camera mounted on a UAV can be used to construct a high-throughput phenotyping platform. One study proposed a QTL localization method for common wheat plant height using UAV imagery (Yan *et al.* 2023), and demonstrated that QTL mapping based on actual plant height measurements and UAV-extracted data yielded highly consistent results. Similarly, research using red, green, and blue (RGB) images for sorghum plant height extraction found that UAV-estimated plant height aligned well with traditional genomic prediction models (Watanabe *et al.* 2017). In addition, Wang X *et al.* (2019) conducted dynamic QTL mapping with UAV-estimated plant heights and successfully monitored 68 QTLs related to seven plant height traits, which revealed variations in the QTLs responsible for plant height during different fertility periods. Although optical sensors can provide detailed information about the surface characteristics of the vegetation canopy, they cannot capture changes in canopy structure, so it is difficult to acquire three-dimensional information. This limitation often leads to saturation at high biomass levels or in dense vegetation. In contrast, LiDAR technology can acquire and measure the vertical structure of tree canopies and generate an accurate 3D point cloud of the object (Popescu 2007; Qin *et al.* 2015). This avoids the issue of vegetation index saturation in optical remote sensing (Cook *et al.* 2009; Karna *et al.* 2015). Currently, LiDAR is widely used for plant height inversion, and it has achieved more accurate estimations (Luo *et al.* 2017; Madec *et al.* 2017; Zhou *et al.* 2020). Studies have shown that UAV-based LiDAR systems provide more precise estimates of plant height than UAV-based RGB cameras (Luo *et al.* 2017; Madec *et al.* 2017). Therefore, LiDAR sensor-based inversion of plant height is more suitable for complex environments involving multiple varieties and fertility periods, as well as small unit area plantings. This approach holds significant promise for estimating maize plant height in the field for QTL localization in genetic analysis.

In this study, UAV-based LiDAR sensor data were used to map QTLs for maize plant height using two populations of doubled haploid (DH) lines. Conducted in two different environments, this study employed a UAV equipped with

a LiDAR sensor for data collection. Leveraging two high-density genetic maps, inclusive composite interval mapping was applied to validate the accuracy of the UAV LiDAR data in phenotyping and assess its utility in crop genetic improvement. This study aims to: 1) identify the best predictors of plant height in field breeding experiments; 2) construct two high-density genetic maps; and 3) evaluate the accuracy and utility of UAV remote sensing data for the QTL mapping of plant height in breeding trials. The findings highlight the importance and feasibility of UAV-based LiDAR for high-throughput and accurate phenotyping. This study lays a theoretical foundation for addressing the challenges associated with large-scale, accurate phenotyping in practical maize genetic breeding trials.

2. Materials and methods

2.1. Test materials and study design

This study used the nationally recognized maize variety Zhongdan 909 (Zheng58×HD568) as the primary source material. DH lines were generated by inducing and constructing populations from their F_1 and F_2 generation plants. The resulting DH line populations from the F_1 and F_2 generations consisted of 113 and 157 lines, respectively, numbered sequentially from 1 to 270. Field trials were conducted in two locations: Sanya, Hainan Province and Xinxiang, Henan Province, China (Fig. 1). Notably, 10 varieties were absent from replicate 2 in the Sanya test area, and 13 varieties were missing in the Xinxiang test area due to unstable seed yields from the selfed lines. Two groups of parental materials were planted at the end of the test area.

Planting commenced on November 25, 2022, at the Sanya Nanfan Base of the Chinese Academy of Agricultural Sciences (CAAS) (Fig. 1-A). This base is located in Yazhou Bay, Sanya City, Hainan Province, and lies in a tropical monsoon climate region (18°36′N, 109°17′E). The area receives an average annual rainfall of 1,100 to 1,300 mm. The climate exhibits distinct wet and dry seasons. Dry conditions prevail from November to April, while the period from July to October is characterized by typhoons and heavy rainfall. The experimental design employed a randomized block trial with two replications. Each family line was planted in single-row plots with individual seeds, spanning 3.5 m in row length. Rows alternated between narrow (0.4 m) and wide (0.8 m) spacing, incorporating high and low ridges. Within each row, plants were spaced 0.25 m apart, totaling 14 plants per row and achieving a planting density of 4,500 plants mu^{-1} (1 mu=666.67 m^2). Field management practices adhered to local standards.

Planting was conducted on June 17, 2023, at the Xinxiang Comprehensive Experimental Base of the Chinese Academy of Agricultural Sciences (Fig. 1-B). This base is located in Qiliying Town, Xinxiang County, Henan Province (35°10′N, 113°47′E), in the temperate monsoon climate zone of the Huang-Huai-Hai Plain, within the Yellow River irrigation region. This region experiences an average annual rainfall of 400 to 800 mm, with rainy and hot seasons primarily occurring from June to August. The experimental setup employed a randomized block design with two replications. Each family line was planted in single-row plots with individual seeds spaced 0.6 m apart and plants within rows spaced 0.25 m apart, totaling 16 plants per row and achieving a planting density of 4,500 plants mu^{-1}. Field management practices followed local standards.

2.2. Image and ground data collection and processing

A DJI M300 RTK UAV equipped with a DJI Zenmuse L1



Fig. 1 Study areas. A, Sanya experimental site, Hainan Province, China. B, Xinxiang experimental site, Henan Province, China. Arrows indicate the variety sorting directions.

sensor (DJI, Shenzhen, China) was used to collect point cloud data, Position and Orientation Systems (POS) data, and images. The UAV operated at a flight altitude of 30 m in equal interval photo mode. To reduce motion blur, the shutter speed was configured to 1/1,000 s and the gimbal pitch angle was adjusted to –90°, to ensure vertical downward image capture. The UAV flew at a speed of 2.4 m s^{-1} with a route overlap rate of 75% and a heading overlap rate of 80%.

High-precision point cloud data were collected at a height of 30 m on several dates in 2023 under clear skies: February 19 (milk stage, Sanya), July 23 (jointing stage, Xinxiang), July 30 (12th leaf stage, Xinxiang), August 5 (tasseling stage, Xinxiang), August 15 (silking stage, Xinxiang), and August 22 (milk stage). The images were stitched together using Agisoft Metashape (Agisoft LLC, Russia). For LiDAR data preprocessing, DJI Terra software was employed. The POS data and digital images were imported to generate point clouds in LAS format with the WGS 84/UTM zone 49N projected coordinate system.

Statistical variables derived from DSM and DTM were used to estimate maize plant height through regional analysis using ArcGIS 10.8 software. Vector boundaries were delineated to define the experimental plot areas and aid in cropping the plot images to identify the region of interest (ROI). Elevation values for the ground and the canopy top were extracted from the DSM and DTM statistics within the ROI. The height of the maize plants was estimated as the difference between these two values.

$$MH_{UAV(m,n)}=DSM_m-DTM_n \quad (1)$$

where MH_{UAV} denotes the UAV-estimated plant height, m represents the elevation of the upper canopy for variables 05 to 12 in Table 1, and n corresponds to the ground elevation for variables 01 to 04 in Table 1.

The selection of ROIs significantly influences the extraction of statistical values from plots. Two methods were used for ROI selection in maize plant height estimation: (1) plot-based selection (row) and (2) single maize plant-based selection (single). Using data from Sanya, MH_{UAV} was calculated separately for all combinations of variables to determine the optimal variables for precise plant height estimation.

During point cloud data collection, five representative maize plants from replicate 1 trial plots were randomly selected to measure their plant height and validate the accuracy of UAV-estimated plant height (MH_{UAV}) data. Plant height measurements were obtained using a telescopic tower ruler to record the average height of the maize plants as the mean plant height (MH_{obs}) for the surveyed plots. The height measurement spanned from the highest point of natural growth to the base of the plant. To assess the accuracy of plant height estimation, the coefficient of determination (R^2), root mean square error (RMSE), and relative root mean square error (rRMSE) were calculated using the following eqs.:

$$R^2=1-\frac{\sum_{i=1}^{n}(\hat{y}_i-y_i)^2}{\sum_{i=1}^{n}(\bar{y}_i-y_i)^2} \quad (2)$$

$$\text{RMSE}=\sqrt{\frac{1}{n}\sum_{i=1}^{n}(y_i-\hat{y}_i)^2} \quad (3)$$

$$\text{rRMSE}\ (\%)=\frac{\text{RMSE}}{\bar{y}}\times 100 \quad (4)$$

where $\hat{y}_i$ represents the estimated plant height value for the i-th sample collected through UAV remote sensing (MH_{UAV}), y_i represents the actual field measurements of plant height for the i-th sample, and $\bar{y}_i$ represents the average plant height of all the field measurements.

The maize plant height was batch-estimated and the accuracy was evaluated. The UAV LiDAR data acquired in Sanya, along with the actual measured plant height data, were used for training. The quantile with the smallest relative rRMSE was selected as the best estimate for maize plant height, which was then used to establish the maize plant height estimation method. The UAV LiDAR data acquired in Xinxiang, along with the field-measured plant height data, were used for validation and QTL analysis.

2.3. High-density genetic map construction and QTL mapping

In this study, leaf samples from the F_1DH, F_2DH, and parental plants were collected 40 days after planting. High-quality genomic DNA was extracted from the population using the hexadecyl trimethyl ammonium bromide (CTAB) method. The concentration and purity of DNA samples were assessed

Table 1 Variables for estimating maize plant height

Input[1)]	ROI[2)]	Variable	Name	Definition	Type
DTM	Row	01	MIN	The minimum value of DTM in the row	Ground elevation
		02	MAX	The maximum value of DTM in the row	
		03	MEAN	The average value of DTM in the row	
		04	MEDIAN	The median DTM in the row	
DSM		05	MAX_row	The maximum value of DSM in the row	Canopy top elevation
		06	PCT99_row	The 99th percentile of DSM in the row	
		07	PCT98_row	The 98th percentile of DSM in the row	
		08	PCT95_row	The 95th percentile of DSM in the row	
	Single	09	MAX_aver	Average of maximum values in single plant	
		10	PCT99_aver	Average of the 99th percentile in single plant	
		11	PCT98_aver	Average of the 98th percentile in single plant	
		12	PCT95_aver	Average of the 95th percentile in single plant	

[1)] DTM, Digital Terrain Model; DSM, Digital Surface Model.
[2)] ROI, region of interest. The “row” and “single” represent the plot and single plant scale, respectively.

using a NanoDrop 2000 spectrophotometer and further confirmed through 1% agarose gel electrophoresis to ensure that the samples met quality criteria of a DNA concentration exceeding 20 ng μL^{-1}, a purity index (OD_{280}/OD_{260} value) between 1.70 and 1.90, and displaying a single, bright band without contaminants. DNA samples meeting these criteria were then submitted for SNP genotyping.

A total of 310 materials were genotyped using 48K liquid phase capture sequencing. SNP markers of the two populations were filtered, and deleted if they met any the following criteria: (1) SNP markers without polymorphism in both parents; (2) SNP markers with heterozygous parents; (3) SNP markers with a deletion rate greater than 10%; (4) SNP markers with heterozygosity greater than 10%; (5) SNP markers with a minor allele frequency (MAF) less than 0.05; and (6) SNP markers that did not conform to a 1:1 ratio in a Chi-square test. The genotypes of the samples were then analyzed according to these criteria: (1) Individuals with a marker deletion rate greater than 10% were deleted; and (2) individuals with marker heterozygosity rates greater than 20% were deleted.

Based on the filtered SNP markers, bin markers of the F_1DH and F_2DH populations were screened using the sliding window approach, and a bin map was constructed. The method is as follows: a window of 15 adjacent SNP markers is moved one SNP marker at a time. If more than 11 SNP markers within the window are from the same parent, they are regarded as homozygous sites; otherwise, they are considered heterozygous sites. Adjacent windows with the same genotypes are merged into one fragment, and differences in genotypes between fragments indicate the presence of recombination sites. Contiguous fragments without recombination are specified as one bin marker. R/ASMap was then used to construct the genetic linkage map.

QTL localization was performed using ICIMapping. The ICIM-ADD method was chosen for maize plant height QTL localization in the DH line populations, with the LOD value set to 2.5 and other settings left at default values. The results were assessed based on the phenotypic variance explained (PVE) value and LOD to identify the plant height QTLs. A nomenclature convention was followed by naming each QTL as q+trait abbreviation+chromosome number. For example, a QTL detected on chromosome 1 would be named *qPH1-1*, with *1-1* indicating the first QTL set on chromosome 1.

Overall, UAV LiDAR sensors were used to monitor maize plant height in the field. The best statistical variables were selected and a method for UAV-estimated plant height was developed. The QTL analysis of UAV-estimated plant height was performed using the inclusive composite interval mapping method in conjunction with high-density genetic mapping. The overall workflow of this study is shown in Fig. 2.

3. Results

3.1. Optimal UAV-based plant height estimation

The data from Sanya were analyzed to identify the optimal variables for estimating plant height. MH_{UAV} was calculated using various combinations of variables at both the row scale

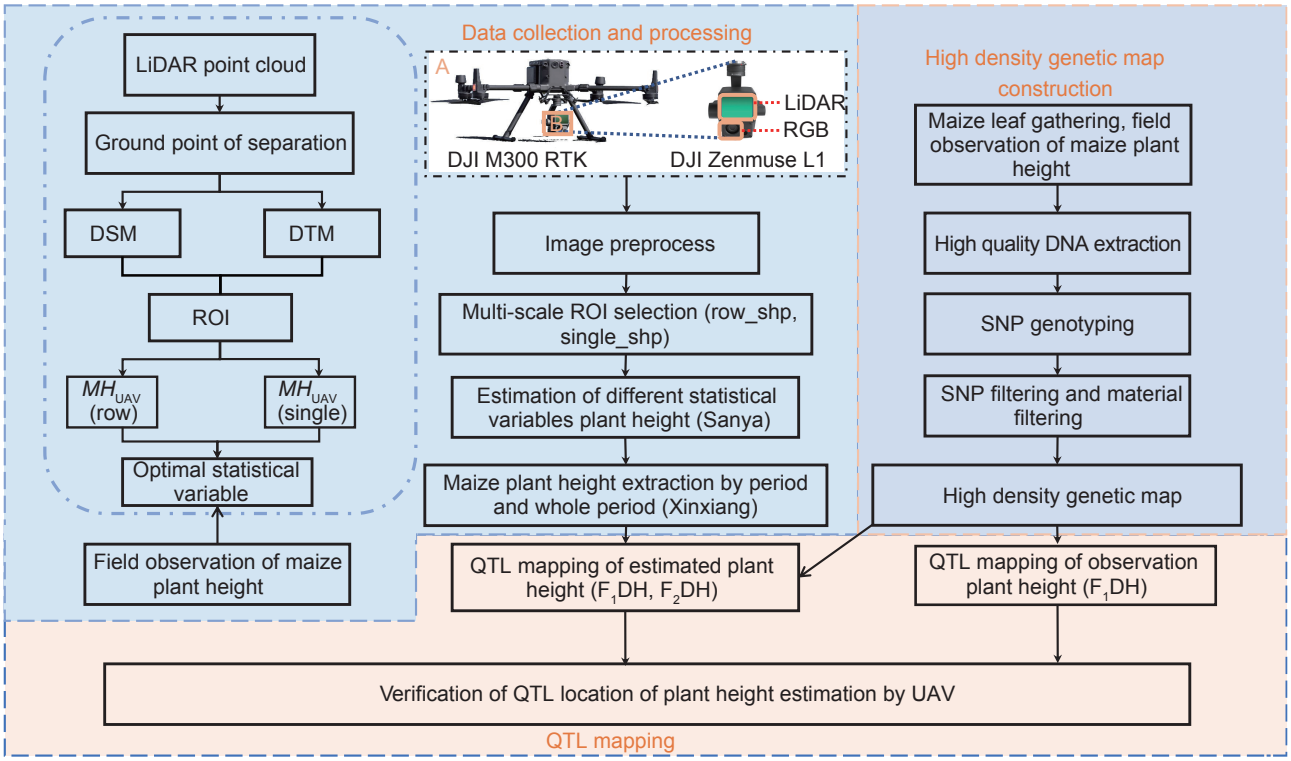


Fig. 2 Experimental design flow chart. A, the black dotted box indicates unmanned aerial vehicle (UAV) remote sensing platforms and sensors. B, light detection and ranging (LiDAR) module and RGB module. DSM, Digital Surface Model; DTM, Digital Terrain Model; ROI, region of interest. MH_{UAV}, UAV-estimated plant height.

and the single-plant scale. The resulting RMSE matrix for plant height estimation is shown in Fig. 3. Generally, single-plant scale estimation demonstrated superior performance compared to plot scale estimation. The RMSE exhibited minimal variation along the vertical axis (where "*n*" indicates the ground elevation value), while more substantial differences were observed along the horizontal axis (where "m" denotes the elevation of the canopy top). This suggests that variable "*m*", representing the elevation of the canopy top, exerts a greater influence on the accuracy of plant height estimation than variable "*n*", which represents the ground elevation value.

At the row scale, using the variable PCT99_row for MH_{UAV} demonstrated greater precision, with an R^2 value of 0.56, an RMSE value of 0.17, and an rRMSE value of 0.12, surpassing the variables MAX_row, PCT98_row, and PCT95_row (RMSE range: 0.20–0.51 m; refer to Appendix A for detailed fitting results). At the single-plant scale, MH_{UAV} demonstrated greater precision using the variable MAX_aver (Fig. 4-A), which achieved a fitted R^2 value of 0.67, an RMSE value of 0.12, and an rRMSE value of 0.07 compared to the variables PCT99_aver, PCT98_aver, and PCT95_aver (RMSE range: 0.13–0.52 m). This study demonstrated that R^2, RMSE, and rRMSE values were significantly higher at the single-plant scale compared to the row scale. Therefore, MAX_aver and MIN fit were identified as the most effective statistical variables for UAV-based plant height estimation in this study.

The optimal combination of variables for estimating plant height was selected based on the best statistical variables identified in Sanya. Then the fittings for MH_{UAV} and MH_{obs} in Xinxiang were generated to explore the relationship across the five growth periods, which revealed substantial variations in plant heights at different developmental stages. The results of estimating maize plant height in Xinxiang using the identified optimal parameters and the estimation accuracy

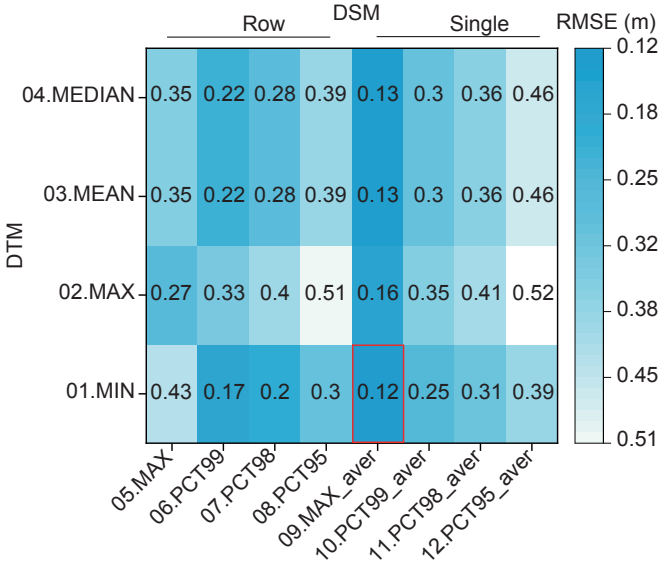


Fig. 3 Estimating root mean square error (RMSE) of plant height using combinations of different variables. At the individual plant scale, MAX_aver estimated plant height with the best accuracy (RMSE: 0.12 m), which is highlighted with a red box. DSM, Digital Surface Model; DTM, Digital Terrain Model.

for each period are depicted in Fig. 5. For the five growth periods, the R^2 values were 0.30, 0.27, 0.55, 0.66, and 0.82, with corresponding RMSE values of 0.14, 0.19, 0.23, 0.33, and 0.26, and rRMSE values of 0.23, 0.28, 0.22, 0.23, and 0.17, respectively.

Note that a typhoon passed through the day before data collection on July 30, 2023, causing the collapse of some maize plants. In addition, when combining and fitting data from the five growth periods covering the full reproductive period in Xinxiang, the R^2 value reached a maximum of 0.88, and the rRMSE was 0.15 (Fig. 5-E).

3.2. High-density genetic map construction and phenotypic evaluation

The numbers of remaining SNP markers in the F_1DH and F_2DH populations were 85,907 and 83,534, respectively, with population sizes of 99 and 153, respectively. These SNP markers were evenly distributed across the 10 maize chromosomes. Using the sliding window strategy, 1,577 and 2,197 bin markers were obtained for the F_1DH and F_2DH populations, respectively. Details of these maps are presented in Fig. 6. In the F_1DH population, the genetic map had a total length of 1,715.08 cM with an average genetic distance of 1.09 cM. For the F_2DH population, the total length of the genetic map was 2,213.89 cM and the average genetic distance was 1.27 cM (Appendices B and C). Significant correlations between genetic distance and physical distance were found in both populations, with coefficients of 0.92 and 0.93 (Appendix D). In addition, the collinearity between genetic and physical distances indicated that most bin markers were arranged in an order consistent with the physical maps. These results indicate a strong correlation between the genetic and physical distances in the genetic linkage maps (Appendices D and E). Overall, the genetic linkage maps demonstrate high accuracy and are well-suited for subsequent analyses.

Based on traditional field measurements, a basic descriptive statistical analysis of plant height data from two environments, Sanya and Xinxiang, was conducted. This analysis revealed that the plant height of HD568 exceeded that of Zheng58 after the tasseling stage, which meets the criteria for seed production and can assist in the selection of favorable combinations. In addition, the results indicated that the slow growth period occurred from August 15 to August 21, while the rapid growth period was from July 23 to August 15 (Table 2). On July 23, maize was at the jointing stage, and by August 15, some maize had reached the tasseling stage. This indicates that the period from the jointing stage to the tasseling stage is a phase of rapid growth. The coefficient of variation for MH_{obs} (August 22, Xinxiang) sown in 2023 was 20.68%. Further analysis of variance for plant height showed highly significant differences among the genotypes (Table 3), indicating that these differences are likely due to genetic factors.

The distribution of maize plant height across various environments followed the typical pattern of a quantitative trait distribution (Fig. 7-A). A notable linear correlation was observed between the maize plant heights in different

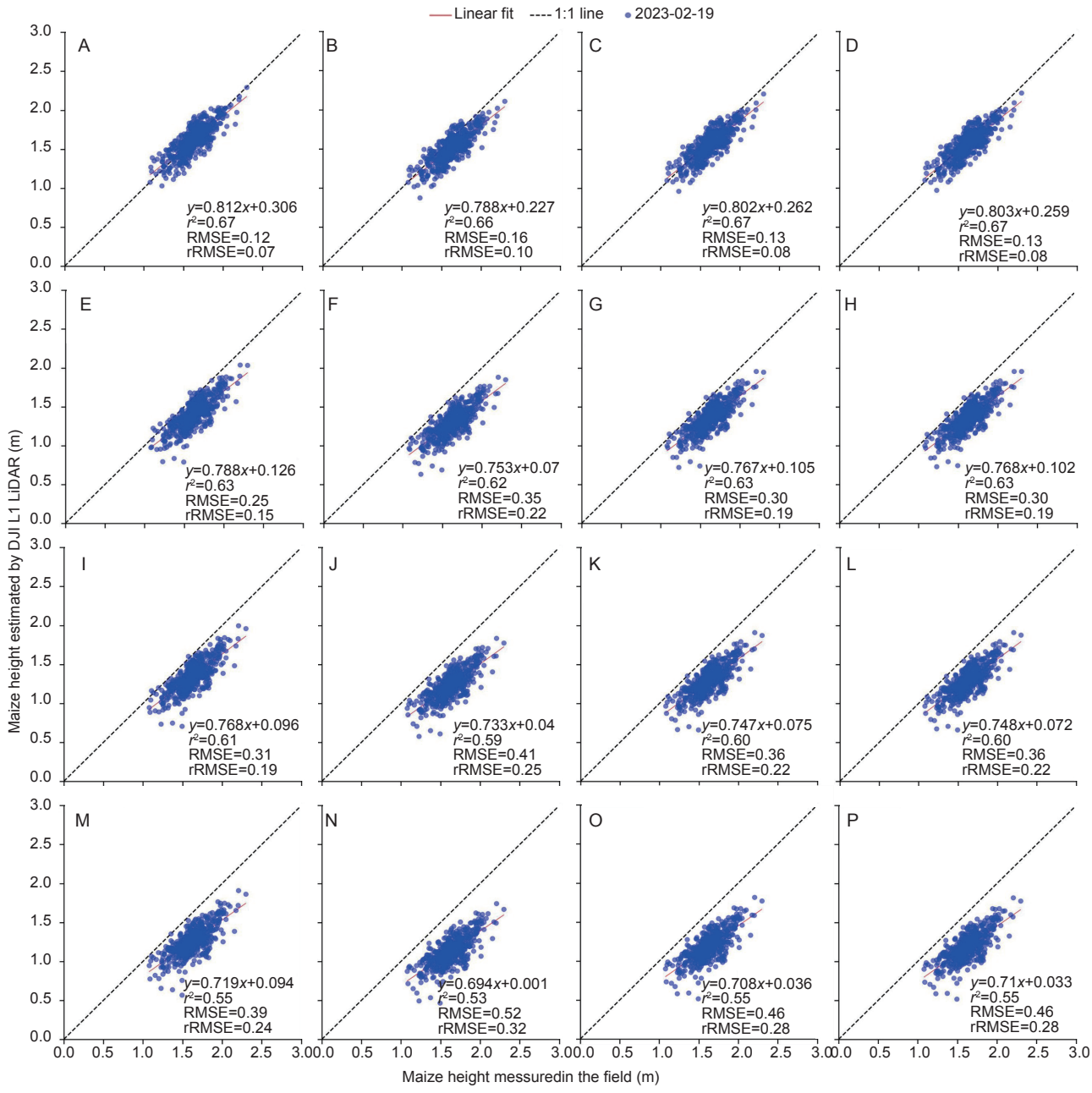


Fig. 4 Fitting results based on combinations of different variables at the single-plant scale (Sanya, Hainan Province, China). A, MAX_aver and MIN fit results. B, MAX_aver and MAX fit results. C, MAX_aver and MEAN fit results. D, MAX_aver and MEDIAN fit results. E, PCT99_aver and MIN fit results. F, PCT99_aver and MAX fit results. G, PCT99_aver and MEAN fit results. H, PCT99_aver and MEDIAN fit results. I, PCT98_aver and MIN fit results. J, PCT98_aver and MAX fit results. K, PCT98_aver and MEAN fit results. L, PCT98_aver and MEDIAN fit results. M, PCT95_aver and MIN fit results. N, PCT95_aver and MAX fit results. O, PCT95_aver and MEAN fit results. P, PCT95_aver and MEDIAN fit results. LiDAR, light detection and ranging. For all R^2 values, P<0.001.

environments, with a correlation coefficient of 0.62 (Fig. 7-B). Significant variations in plant height were also evident across the different developmental stages, with correlations ranging from 0.18 to 0.83. These findings suggest a shared genetic basis for plant height within this population that is consistent across diverse environments and developmental stages. However, it is important to recognize that environmental conditions also influence maize plant height to some extent, and this influence interacts with genetic factors.

3.3. QTL mapping of maize plant height

Given the observed differences between MH_{obs} and MH_{UAV} in various environments and reproductive periods, QTL localization for plant height was conducted in the F_1DH population. This analysis compared the manually measured plant height with the UAV-estimated plant height to validate the feasibility of using UAV phenotypic data for genetic breeding. The results, shown in Fig. 8, identified 12 QTLs associated with plant height in the F_1DH population. These loci were distributed across chromosomes 1, 2, 3, 6, and 10, with

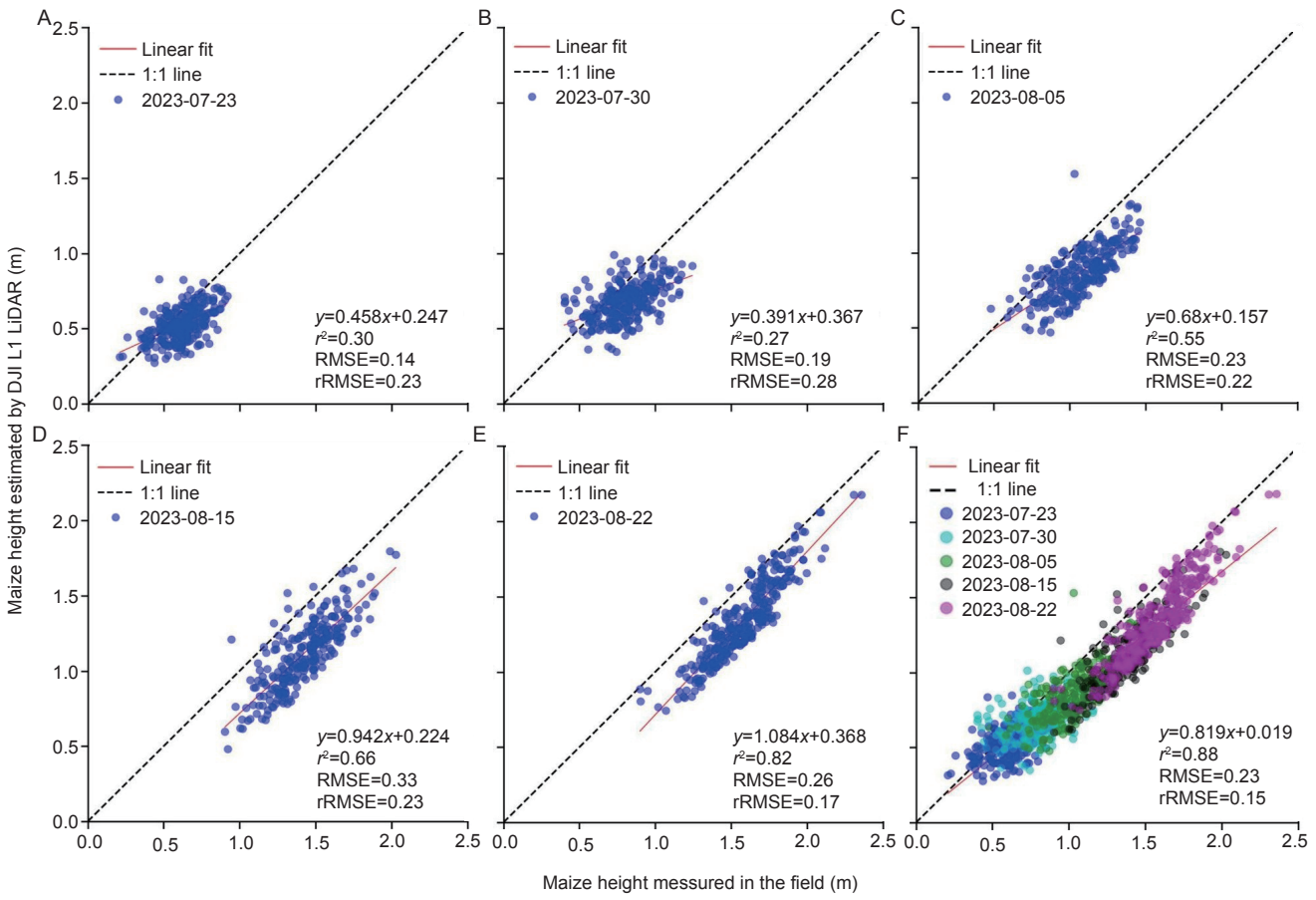


Fig. 5 Estimated accuracy of each growth period. Fitting was obtained from the best statistical variables, single plant scale: MAX_aver and MIN. LiDAR, light detection and ranging. For all r^2 values, $P<0.001$.

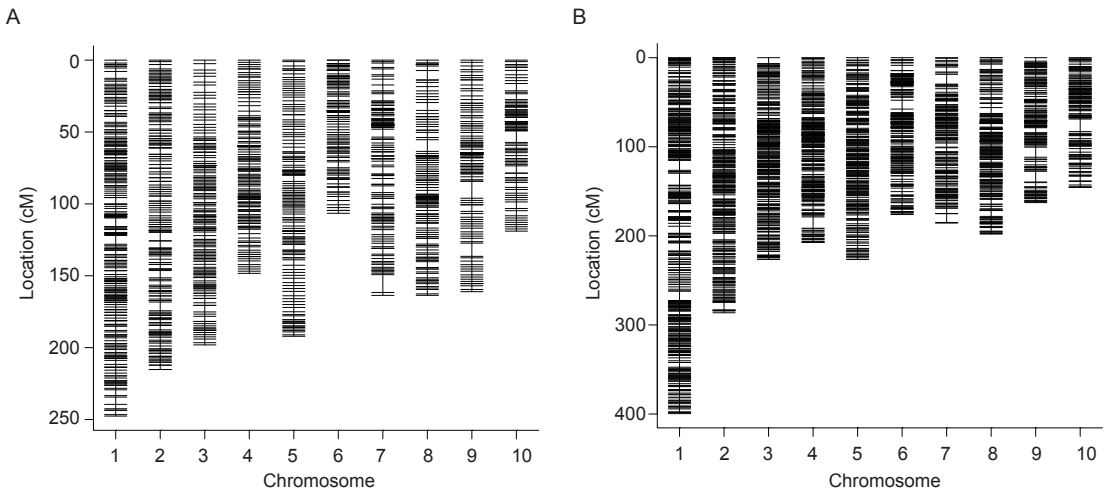


Fig. 6 Genetic mapping information. A, high-density genetic map of the F_1DH population. B, high-density genetic map of the F_2DH population.

detailed information provided in Appendix F. The phenotypic contribution rates of individual QTLs ranged from 12.60 to 22.55%, with all values exceeding 10%, indicating that these QTLs are the primary regulators of plant height. Plant height is mainly controlled by distinct QTLs at different reproductive stages. For example, at the nodulation and small trumpet stages (July 30, 2023 and August 5, 2023), several QTLs influencing maize plant height at multiple stages were localized to the same locus, i.e., locus 184 (*qPH3-3*) on chromosome 3. Most other QTLs had similar loci in different environments and reproductive periods. For instance, the QTLs *qPH3-5* and *qPH3-6* had overlapping positions at 196–197 Mb

Table 2 Basic description of maize height (MH_{obs}) of the doubled haploid population and its parents

Date	Parent		Doubled haploid population[1)]				
	Zheng58 (cm)	HD568 (cm)	Mean (cm)	Minimum (cm)	Maximum (cm)	SD (cm)	CV (%)
February 19	157.67	173.00	161.59	94.25	215.40	19.35	11.97
July 23	59.53	88.37	61.33	22.87	91.67	13.01	21.22
July 30	72.90	104.83	80.61	40.10	124.33	16.38	20.32
August 5	89.33	141.33	107.61	47.88	147.67	18.79	17.46
August 15	108.70	149.27	142.17	90.33	202.77	20.07	14.12
August 22	159.00	170.33	155.27	90.33	230.67	20.68	13.32

[1)] SD is standard deviation; CV represents the coefficient of variation.

Table 3 Two-factor variance analysis of maize height

	Sum square	*df*	Mean square	*F*	*P*-value
Genotype	164,815	253	651.40	4.32	$2.20\times10^{-16***}$
Environment	5,073	1	5,072.80	33.67	$1.94\times10^{-8***}$
Residual	38,113	253	150.60		

*** indicates extremely significant correlation at the 0.001 level.

within 1-LOD support intervals, and their PVEs for MH_{obs} and MH_{UAV} were also similar. In addition, using MH_{UAV} for localization revealed the same loci on chromosomes 2, 3, and 6 that were identified with the actual plant heights (*qPH2-3*, *qPH3-3*, *qPH3-4*, and *qPH6-1*), with PVEs of 15.13, 14.05, 18.75, and 17.45%, respectively.

In the F_2DH population (Fig. 9), the QTL localization identified 20 QTLs associated with plant height. These QTLs were distributed across chromosomes 1, 2, 3, 4, 5, 6, 8, and 9, with detailed information in Appendix G. Similar loci on chromosome 6 (120, 124, 129, and 130) were observed during four different reproductive periods, with PVEs of 16.61, 9.33, 9.63, and 9.59%. The same locus (103) and a similar locus (100) on chromosome 9 were observed during critical growth periods (July 30, August 5, and August 15, 2023), with PVEs of 11.17, 13.74, and 12.38%. In total, 32 QTLs related to plant height were detected in the F_1DH and F_2DH populations, with 27 of these QTLs identified using UAV data. However, no QTL overlap was observed between the two environments.

4. Discussion

4.1. UAV LiDAR sensor-based maize plant height estimation

In this study, a UAV-based LiDAR sensor was used to estimate plant height for QTL under field trials in a practical breeding scenario. The goal was to establish a method for using UAV remote sensing data to estimate plant height with greater accuracy and stability across various species, reproductive periods, and small-area plantings.

Initially, the stability and accuracy of LiDAR sensor-based plant height estimations at different height fractions were assessed and the statistical variables for estimating maize plant height were identified. As shown in Fig. 6, the findings align with those of previous studies (Malambo *et al.* 2018; Che *et al.* 2020; Shu *et al.* 2022) in that the most accurate plant height estimation at the row scale was achieved using the variables PCT99_row and MIN. This discrepancy may have occurred because MAX_row reflects only the height of

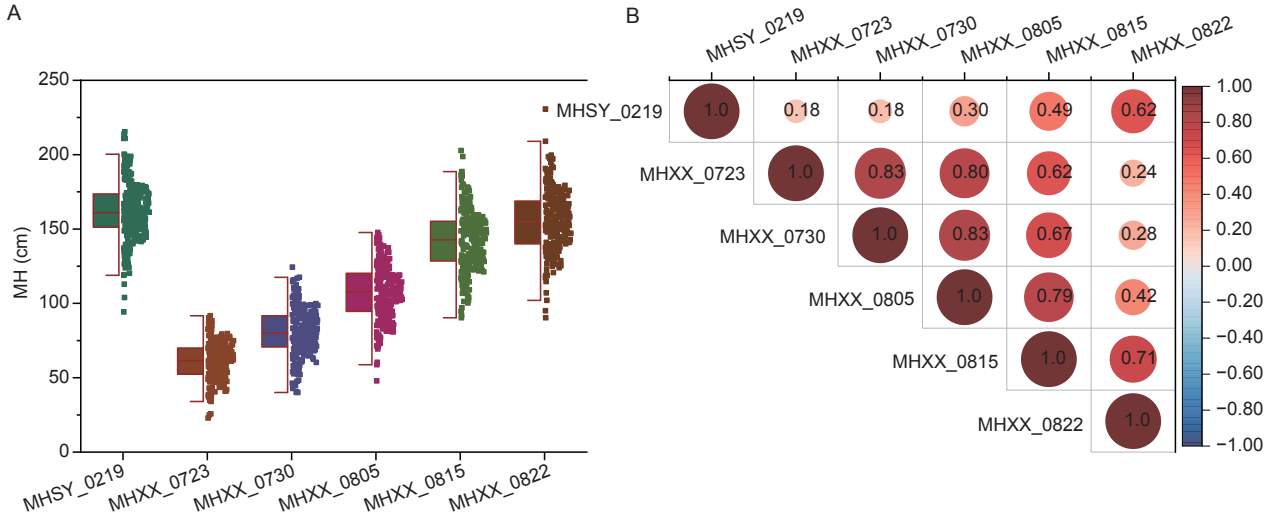


Fig. 7 Distributions and correlations of maize height in different environments. A, maize height data distributions in different periods. Each box represents 25–75% of the data distribution, each error line represents the range within 1.5 interquartile range (IQR), each horizontal line represents the median line, each "–" represents the median, and each "square" represents the plant height. B, the correlations of maize height at each growing stage in the field. Red and blue indicate positive and negative correlations, respectively. The size of each circle is proportional to the correlation coefficient. MH, maize height. SY, Sanya, Hainan Province, China; XX, Xinxiang, Henan Province, China.

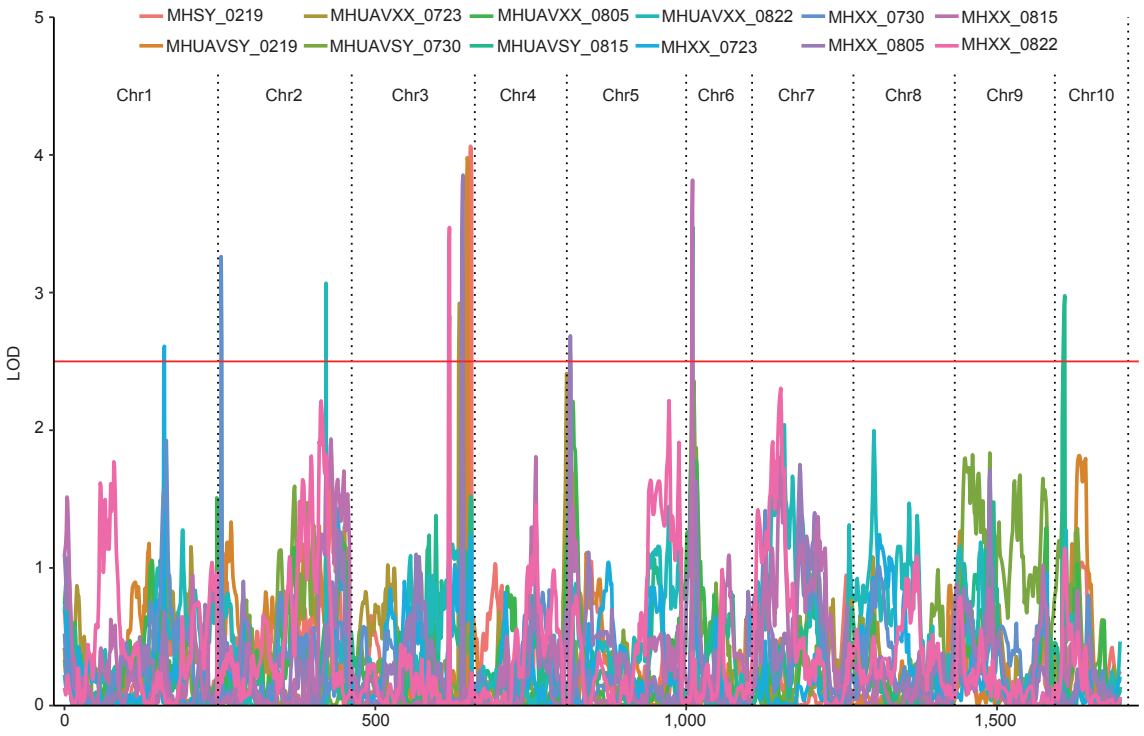


Fig. 8 Locations of QTLs for the F_1DH population in the whole genome. In this study, the LOD was set to 2.5 to indicate the presence of interlocking. MH, maize height. SY, Sanya, Hainan Province, China; XX, Xinxiang, Henan Province, China. UAV, unmanned aerial vehicle; MHUAV, UAV-estimated plant height.

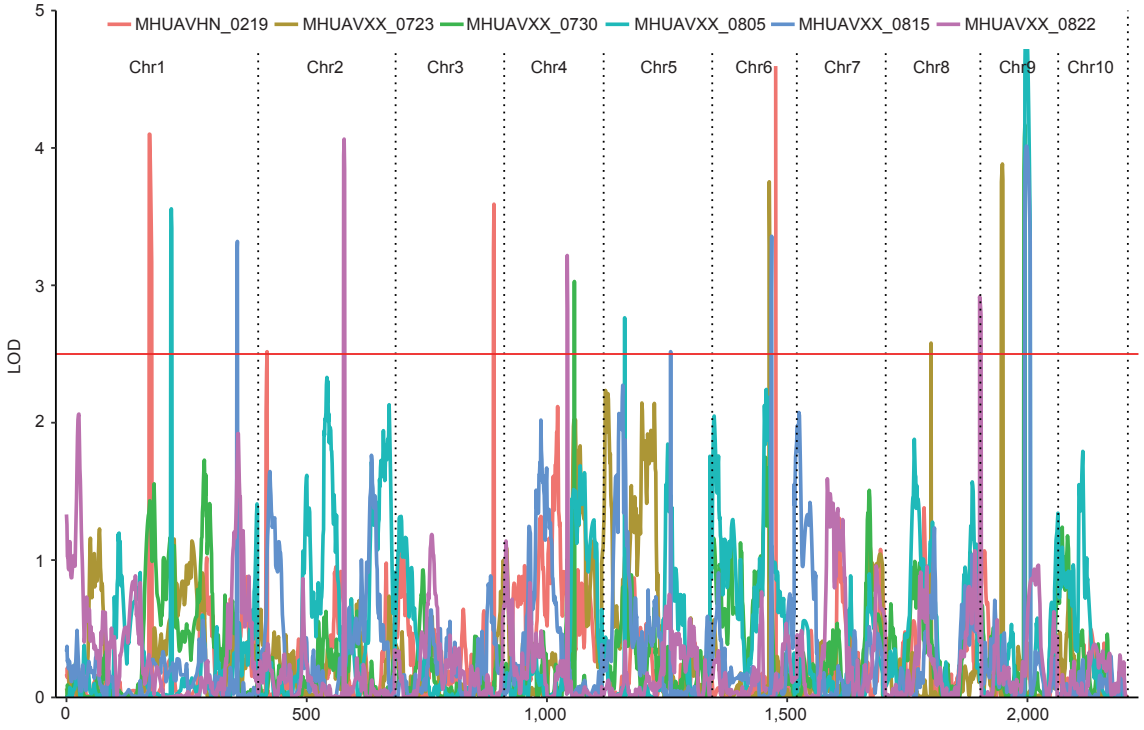


Fig. 9 Locations of QTLs for the F_2DH population in the whole genome. In this study, the LOD was set to 2.5 to indicate the presence of interlocking. MH, maize height. SY, Sanya, Hainan Province, China; XX, Xinxiang, Henan Province, China. UAV, unmanned aerial vehicle; MHUAV, UAV-estimated plant height.

the tallest plant in a row, while field measurements typically involve selecting representative maize plants. Consequently, plant height estimations based on MAX_row often deviate more from the measured values. In addition, airborne LiDAR

data acquisition can be affected by flying birds or insects between the sensor and the canopy top, causing MAX_row to overestimate maize plant height.

At the single-plant scale, averaging variables mitigated the impact of outliers on plant height estimates, leading to higher accuracy. The most precise plant height estimation was obtained with MAX_aver, which represented canopy height (R^2, 0.67; RMSE, 0.12 m; rRMSE, 0.07). This finding is consistent with indoor monitoring platforms, where the highest point in the natural state reflects canopy height. The maximum underestimation occurred during tasseling on August 15, 2023. This underestimation was attributed to the variability of the male spikes, which differ with plant population and variety (Duncan *et al.* 1967). Tasseling was inconsistent among varieties between the F_1DH and F_2DH populations, and the size of the male spike significantly affected plant height estimates. Unstable spike point clouds during model reconstruction may lead to lower plant height estimates (Han *et al.* 2018). Previous studies also found that the length of the male spike impacts plant height measurement (Maresma *et al.* 2016; Shi *et al.* 2016).

As noted, the better accuracy of plant height estimation using single-plant extraction in actual field breeding work validates the feasibility and precision of UAV-based measurements. However, MH_{UAV} is influenced by the size of the male spike, indicating the need for further improvements. For instance, reducing the flight altitude could enhance point cloud density during the tasseling stage.

4.2. Importance of high-density genetic maps

The construction of high-density genetic maps is crucial for precise QTL localization, enhancing efficiency, and improving resolution (Wang Z *et al.* 2019b). The accuracy of genetic mapping, which relies on the discovery of molecular markers and genotyping, directly influences the precision of QTL localization (Wang Z *et al.* 2019a; Liu *et al.* 2020). A low marker density, uneven distribution, and large genetic distances between markers can lead to inaccuracies in QTL localization. Advances in sequencing technology and SNP genotyping on gene chips, which are driven by decreasing costs and rapid bioinformatics development, have revolutionized high-density genetic map construction, and it is now widely applied in genetic analysis (Yu X *et al.* 2020; Lin *et al.* 2021; Lv *et al.* 2021). High-density genetic mapping offers several advantages over low-density mapping. It accurately pinpoints QTL positions, narrows candidate intervals, and enhances localization precision. Moreover, it detects more QTLs and has better sensitivity. In this study, high-density genetic maps were constructed comprising 1,577 and 2,197 high-quality bin markers, respectively (Fig. 6). The average genetic distances between markers were 1.09 and 1.01 cM, respectively. These linkage maps have greater marker densities than several previously reported maps. In addition, the physical interval size for QTL localization was typically 1–2 Mb, with the minimum interval size being 0.86 Mb. This demonstrates that high-density genetic linkage maps can significantly narrow the candidate range (Yang J *et al.* 2020; Ren *et al.* 2022).

4.3. Analysis of the QTL location results of maize plant height

In this study, high-density genetic mapping and MH_{UAV} were used to monitor plant height QTLs. QTL localization was validated in the F_1DH population using field-measured plant height, which confirmed that the loci for UAV-estimated plant height (*qPH2-3*, *qPH3-3*, *qPH3-4*, and *qPH6-1*) were generally consistent with those identified through traditional plant height survey methods. Notably, QTLs that control plant height at multiple reproductive stages were found (Figs. 8 and 9). Three repetitively localized intervals were identified on chromosomes 3, 6, and 9, which contain QTLs such as *qPH3-3*, *qPH3-7*, *qPH6-3*, *qPH6-4*, *qPH6-5*, *qPH9-4*, and *qPH9-5*, suggesting these might be novel loci controlling plant height.

This study also revealed the presence of the candidate gene *ZmWUS1* within the 2.26–3.44 Mb interval on chromosome 2, which is known to regulate maize plant height by controlling meristematic tissue development (Chen *et al.* 2021). Furthermore, the candidate gene *ZmPIN1a* was identified within the 0.06–3.29 Mb interval on chromosome 9, which regulates plant height through auxin transport and accumulation in maize root tips, thereby enhancing root growth while reducing plant height (Li *et al.* 2018). Several QTLs identified in this study, such as *qPH8-1* and *qPH2-4*, overlapped with previously reported QTLs, indicating that they are novel genetic loci contributing to maize plant height control (Li *et al.* 2016; Yang *et al.* 2024). This suggests that certain loci consistently influence plant height across different populations and developmental stages. Most other QTLs exhibited similar loci across the different environments and reproductive periods (*qPH3-2*, *qPH3-3*, *qPH3-4*, and *qPH3-6*), while some QTLs were specific to individual environments, highlighting the strong influence of environmental factors on plant height inheritance. A total of 32 distinct QTLs were monitored throughout the entire reproductive period, and the results indicated that different periods are controlled by different QTLs. This finding is consistent with previous studies showing that various growth stages in maize plant height are influenced by different QTLs (Wang X *et al.* 2019). UAV-estimated plant height, which provides more canopy information, may offer advantages in terms of accuracy and objectivity.

4.4. Factors affecting estimation accuracy

Estimation accuracy can be affected by factors such as the small planting area of the plot, close row spacing between varieties, and leaves obscuring each other in single-row areas. The subjective nature of manual measurement data and variation in results between different individuals further underscore the potential advantages of UAV-estimated plant height data. Also, the timing of high-throughput phenotypic monitoring is crucial for effective data collection and analysis (Shakoor *et al.* 2017). Monitoring multiple reproductive stages has enhanced our understanding of plant developmental processes. Using phenotypic data across multiple fertility periods in genetic mapping enables the identification of a greater number of QTLs influencing the development of

plant height traits. The selection of sampling time points can significantly impact the extraction of phenotypic traits and subsequent analyses, as the QTLs controlling these traits change throughout the growing season. Understanding these variations is essential for analyzing the genetic basis of target traits and improving those traits.

While obtaining UAV-estimated plant height data is feasible and accurate, instances of underestimation still occur (Fig. 3). This could be attributed to the nature of LiDAR, an active remote sensing technology. The sensor emits infrared laser pulses, and the distance to the feature is calculated using the time-of-flight (ToF) method combined with real-time navigation data to determine the spatial location of the feature. During UAV-based LiDAR data collection, especially in the middle and late stages of maize growth when plants are taller and denser, the tops of maize plants are susceptible to wind disturbance. Consequently, infrared laser pulses may not capture the point cloud information as comprehensively as in the early stages.

In this study, LiDAR proved effective in estimating maize plant height for QTLs under complex conditions involving multiple varieties, fertility periods, and small unit area planting. However, its applicability under different conditions, such as varying flight heights, fertilization, flooding, and lodging, remains to be demonstrated. In addition, employing oblique photography has the potential to increase point cloud density, which would enhance the likelihood of detecting the highest point of the plant. This may serve as a compensatory measure for the limited point cloud density of LiDAR and further improve maize height estimation accuracy. Moreover, in actual field breeding experiments, the small unit planting area and the impact of side rows on measurements are often significant. This issue could be addressed by altering planting methods, or by transitioning from single-row to double-row or square layouts, to minimize the influence of neighboring rows on variety-specific measurements and ultimately enhance estimation accuracy.

5. Conclusion

In this study, a UAV high-throughput phenotyping platform equipped with a LiDAR sensor was used to obtain plant height information in the field. By comparing the performance of estimated plant heights at different scales and combining it with a constructed high-density genetic map, the accuracy and stability of plant height estimation at the single-plant scale were better than those at the plot scale. The QTL results based on UAV-estimated single maize plant height values closely matched those derived from observed maize plant height values, highlighting the practicality and feasibility of UAV-based remote sensing technology in gene mining. This study not only provides a method for rapid and efficient plant height monitoring under complex conditions but also lays a theoretical foundation for solving the challenges of large-scale and precise phenotyping in maize genetic breeding trials.

Acknowledgements

This research was supported by the National Key Research and Development Program of China (2023YFD1200500), the National Natural Science Foundation of China (32301395, 42071426, and 51922072), the Nanfan Special Project of the Chinese Academy of Agricultural Sciences (YBXM2305), the Central Public-Interest Scientific Institution Basal Research Fund Program, China (Y2020YJ07 and Y2022XK22), the Key Cultivation Program of the Xinjiang Academy of Agricultural Sciences, China (xjkcpy-2020003), and the Open Competition Project of Heilongjiang Province, China (2021ZXJ05A03).

Declaration of competing interest

The authors declare that they have no conflict of interest.

Declaration of generative AI and AI-assisted technologies in the writing process

The authors declare that they did not use AI in the preparation and writing of this manuscript.

Data availability

All the raw data and code are available from the corresponding authors upon reasonable request.

Appendices associated with this paper are available at https://doi.org/10.1016/j.jia.2024.09.004

References

Araus J L, Kefauver S C, Vergara-Díaz O, Gracia-Romero A, Rezzouk F Z, Segarra J, Buchaillot M L, Chang-Espino M, Vatter T, Sanchez-Bragado R. 2022. Crop phenotyping in a context of global change: What to measure and how to do it. *Journal of Integrative Plant Biology*, **64**, 592–618.

Bai Y, Nie C, Wang H, Cheng M, Liu S, Yu X, Shao M, Wang Z, Wang S, Tuohuti N. 2022. A fast and robust method for plant count in sunflower and maize at different seedling stages using high-resolution UAV RGB imagery. *Precision Agriculture*, **23**, 1720–1742.

Chardon F, Virlon B M, Moreau L, Falque M, Joets J, Decousset L, Murigneux A, Charcosset A. 2004. Genetic architecture of flowering time in maize as inferred from quantitative trait loci meta-analysis and synteny conservation with the rice genome. *Genetics*, **168**, 2169–2185.

Che Y, Wang Q, Xie Z, Zhou L, Li S, Hui F, Wang X, Li B, Ma Y. 2020. Estimation of maize plant height and leaf area index dynamics using an unmanned aerial vehicle with oblique and nadir photography. *Annals of Botany*, **126**, 765–773.

Chen Z, Li W, Gaines C, Buck A, Galli M, Gallavotti A. 2021. Structural variation at the maize WUSCHEL1 locus alters stem cell organization in inflorescences. *Nature Communications*, **12**, 2378.

Cheng M, Jiao X, Liu Y, Shao M, Yu X, Bai Y, Wang Z, Wang S, Tuohuti N, Liu S. 2022. Estimation of soil moisture content under high maize canopy coverage from UAV multimodal data and machine learning. *Agricultural Water Management*, **264**, 107530.

Cook B D, Bolstad P V, Næsset E, Anderson R S, Garrigues S, Morisette J T, Nickeson J, Davis K J. 2009. Using LiDAR and quickbird data to model plant production and quantify uncertainties associated with wetland detection and land cover generalizations. *Remote Sensing of Environment*, **113**, 2366–2379.

Cui D, Cui G, Yang R, She W, Liu Y, Wang H, Su X, Wang J, Liu W, Wang X. 2021. Phenotypic characteristics of ramie (*Boehmeria nivea* L.) germplasm resources based on UAV remote sensing. *Genetic Resources and Crop Evolution*, **68**, 551–566.

Diepenbrock C H, Tang T, Jines M, Technow F, Lira S, Podlich D, Cooper M, Messina C. 2022. Can we harness digital technologies and physiology to hasten genetic gain in US maize breeding? *Plant Physiology*, **188**, 1141–1157.

Du L, Zhang H, Xin W, Ma K, Du D, Yu C, Liu Y. 2021. Dissecting the genetic basis of flowering time and height related-traits using two

doubled haploid populations in maize. *Plants*, **10**, 1585.
Duan T, Zheng B, Guo W, Ninomiya S, Guo Y, Chapman S C. 2016. Comparison of ground cover estimates from experiment plots in cotton, sorghum and sugarcane based on images and ortho-mosaics captured by UAV. *Functional Plant Biology*, **44**, 169–183.
Duncan W G, Williams W A, Loomis R S. 1967. Tassels and the productivity of maize. *Crop Science*, **7**, 37–39.
Fei S, Hassan M A, Xiao Y, Su X, Chen Z, Cheng Q, Duan F, Chen R, Ma Y. 2023. UAV-based multi-sensor data fusion and machine learning algorithm for yield prediction in wheat. *Precision Agriculture*, **24**, 187–212.
Gilliot J, Michelin J, Hadjard D, Houot S. 2021. An accurate method for predicting spatial variability of maize yield from UAV-based plant height estimation: A tool for monitoring agronomic field experiments. *Precision Agriculture*, **22**, 897–921.
Guo F, Hou L, Ma C, Li G, Lin R, Zhao Y, Wang X. 2021. Comparative transcriptome analysis of the peanut semi-dwarf mutant 1 reveals regulatory mechanism involved in plant height. *Gene*, **791**, 145722.
Guo Y, Fu Y H, Chen S, Bryant C R, Li X, Senthilnath J, Sun H, Wang S, Wu Z, de Beurs K. 2021. Integrating spectral and textural information for identifying the tasseling date of summer maize using UAV based RGB images. *International Journal of Applied Earth Observation and Geoinformation*, **102**, 102435.
Han L, Yang G, Yang H, Xu B, Li Z, Yang X. 2018. Clustering field-based maize phenotyping of plant-height growth and canopy spectral dynamics using a UAV remote-sensing approach. *Frontiers in Plant Science*, **9**, 1638.
van Heerwaarden J , Doebley J, Briggs W H, Glaubitz J C, Goodman M M, de Jesus Sanchez Gonzalez J, Ross-Ibarra J. 2011. Genetic signals of origin, spread, and introgression in a large sample of maize landraces. *Proceedings of the National Academy of Sciences of the United States of America*, **108**, 1088–1092.
Hu P, Chapman S C, Wang X, Potgieter A, Duan T, Jordan D, Guo Y, Zheng B. 2018. Estimation of plant height using a high throughput phenotyping platform based on unmanned aerial vehicle and self-calibration: Example for sorghum breeding. *European Journal of Agronomy*, **95**, 24–32.
Jiang Z, Tu H, Bai B, Yang C, Zhao B, Guo Z, Liu Q, Zhao H, Yang W, Xiong L. 2021. Combining UAV-RGB high-throughput field phenotyping and genome-wide association study to reveal genetic variation of rice germplasms in dynamic response to drought stress. *New Phytologist*, **232**, 440–455.
Jin X, Zarco-Tejada P J, Schmidhalter U, Reynolds M P, Hawkesford M J, Varshney R K, Yang T, Nie C, Li Z, Ming B. 2021. High-throughput estimation of crop traits: A review of ground and aerial phenotyping platforms. *IEEE Geoscience and Remote Sensing Magazine*, **9**, 200–231.
Karna Y K, Hussin Y A, Gilani H, Bronsveld M, Murthy M, Qamer F M, Karky B S, Bhattarai T, Aigong X, Baniya C B. 2015. Integration of WorldView–2 and airborne LiDAR data for tree species level carbon stock mapping in Kayar Khola watershed, Nepal. *International Journal of Applied Earth Observation and Geoinformation*, **38**, 280–291.
Kumar P, Choudhary M, Halder T, Prakash N R, Singh V, Vineeth T V, Sheoran S, Longmei N, Rakshit S, Siddique K H. 2022. Salinity stress tolerance and omics approaches: Revisiting the progress and achievements in major cereal crops. *Heredity*, **128**, 497–518.
Li X, Zhou Z, Ding J, Wu Y, Zhou B, Wang R, Ma J, Wang S, Zhang X, Xia Z. 2016. Combined linkage and association mapping reveals QTL and candidate genes for plant and ear height in maize. *Frontiers in Plant Science*, **7**, 833.
Li Z, Zhang X, Zhao Y, Li Y, Zhang G, Peng Z, Zhang J. 2018. Enhancing auxin accumulation in maize root tips improves root growth and dwarfs plant height. *Plant Biotechnology Journal*, **16**, 86–99.
Lin Y, Jiang X, Hu H, Zhou K, Wang Q, Yu S, Yang X, Wang Z, Wu F, Liu S. 2021. QTL mapping for grain number per spikelet in wheat using a high-density genetic map. *The Crop Journal*, **9**, 1108–1114.
Liu M, He W, Zhang A, Zhang L, Sun D, Gao Y, Ni P, Ma X, Cui Z, Ruan Y. 2021. Genetic analysis of maize shank length by QTL mapping in three recombinant inbred line populations. *Plant Science*, **303**, 110767.
Liu S, Jin X, Nie C, Wang S, Yu X, Cheng M, Shao M, Wang Z, Tuohuti N, Bai Y. 2021. Estimating leaf area index using unmanned aerial vehicle data: Shallow vs. deep machine learning algorithms. *Plant Physiology*, **187**, 1551–1576.
Liu T, He J, Dong K, Wang X, Wang W, Yang P, Ren R, Zhang L, Zhang Z, Yang T. 2020. QTL mapping of yield component traits on bin map generated from resequencing a RIL population of foxtail millet (*Setaria italica*). *BMC Genomics*, **21**, 1–13.
Lu J, Cheng D, Geng C, Zhang Z, Xiang Y, Hu T. 2021. Combining plant height, canopy coverage and vegetation index from UAV-based RGB images to estimate leaf nitrogen concentration of summer maize. *Biosystems Engineering*, **202**, 42–54.
Lu L, Luo J, Xin Y, Duan H, Sun Z, Qiu Y, Xiao Q. 2022. How can UAV contribute in satellite-based Phragmites australis aboveground biomass estimating? *International Journal of Applied Earth Observation and Geoinformation*, **114**, 103024.
Luo S, Liu W, Zhang Y, Wang C, Xi X, Nie S, Ma D, Lin Y, Zhou G. 2021. Maize and soybean heights estimation from unmanned aerial vehicle (UAV) LiDAR data. *Computers and Electronics in Agriculture*, **182**, 106005.
Luo S, Wang C, Xi X, Pan F, Qian M, Peng D, Nie S, Qin H, Lin Y. 2017. Retrieving aboveground biomass of wetland Phragmites australis (common reed) using a combination of airborne discrete-return LiDAR and hyperspectral data. *International Journal of Applied Earth Observation and Geoinformation*, **58**, 107–117.
Lv D, Zhang C, Yv R, Yao J, Wu J, Song X, Jian J, Song P, Zhang Z, Han D. 2021. Utilization of a wheat50K SNP microarray-derived high-density genetic map for QTL mapping of plant height and grain traits in wheat. *Plants*, **10**, 1167.
Madec S, Baret F, De Solan B, Thomas S, Dutartre D, Jezequel S, Hemmerlé M, Colombeau G, Comar A. 2017. High-throughput phenotyping of plant height: Comparing unmanned aerial vehicles and ground LiDAR estimates. *Frontiers in Plant Science*, **8**, 2002.
Malambo L, Popescu S C, Murray S C, Putman E, Pugh N A, Horne D W, Richardson G, Sheridan R, Rooney W L, Avant R. 2018. Multitemporal field-based plant height estimation using 3D point clouds generated from small unmanned aerial systems high-resolution imagery. *International Journal of Applied Earth Observation and Geoinformation*, **64**, 31–42.
Maresma Á, Ariza M, Martínez E, Lloveras J, Martínez-Casasnovas J A. 2016. Analysis of vegetation indices to determine nitrogen application and yield prediction in maize (*Zea mays* L.) from a standard UAV service. *Remote Sensing*, **8**, 973.
Popescu S C. 2007. Estimating biomass of individual pine trees using airborne lidar. *Biomass and Bioenergy*, **31**, 646–655.
Pugh N A, Horne D W, Murray S C, Carvalho Jr G, Malambo L, Jung J, Chang A, Maeda M, Popescu S, Chu T. 2018. Temporal estimates of crop growth in sorghum and maize breeding enabled by unmanned aerial systems. *The Plant Phenome Journal*, **1**, 1–10.
Qin Y, Li S, Vu T T, Niu Z, Ban Y. 2015. Synergistic application of geometric and radiometric features of LiDAR data for urban land cover mapping. *Optics Express*, **23**, 13761–13775.
Radanović S N, Živanović T B, Sečanski M D, Jovanović S V, Prodanović S A, Šurlan M G G. 2015. The genetic basis of inheritance of plant height in maize. *Journal of Agricultural Sciences* (Belgrade), **60**, 97–107.
Ren J, Zhang X, Li Z, Wu P. 2022. Genetic analysis of maternal haploid inducibility for in vivo haploid induction in maize. *Agriculture*, **12**, 845.
Rodene E, Xu G, Palali Delen S, Zhao X, Smith C, Ge Y, Schnable J, Yang J. 2022. A UAV-based high-throughput phenotyping approach to assess time-series nitrogen responses and identify trait-associated genetic components in maize. *The Plant Phenome Journal*, **5**, e20030.
Shakoor N, Lee S, Mockler T C. 2017. High throughput phenotyping to accelerate crop breeding and monitoring of diseases in the field. *Current Opinion in Plant Biology*, **38**, 184–192.
Shi Y, Thomasson J A, Murray S C, Pugh N A, Rooney W L, Shafian S, Rajan N, Rouze G, Morgan C L, Neely H L. 2016. Unmanned aerial vehicles for high-throughput phenotyping and agronomic research. *PLoS ONE*, **11**, e0159781.
Shiferaw B, Smale M, Braun H J, Duveiller E, Reynolds M, Muricho G. 2013. Crops that feed the world 10. Past successes and future challenges to the role played by wheat in global food security. *Food Security*, **5**, 291–317.
Shu M, Shen M, Dong Q, Yang X, Li B, Ma Y. 2022. Estimating the maize above-ground biomass by constructing the tridimensional concept model based on UAV-based digital and multi-spectral

images. *Field Crops Research*, **282**, 108491.
Teng F, Zhai L, Liu R, Bai W, Wang L, Huo D, Tao Y, Zheng Y, Zhang Z. 2013. ZmGA3ox2, a candidate gene for a major QTL, *qPH3.1*, for plant height in maize. *The Plant Journal*, **73**, 405–416.
Veldboom L R, Lee M. 1996. Genetic mapping of quantitative trait loci in maize in stress and nonstress environments: I. Grain yield and yield components. *Crop Science*, **36**, 1310–1319.
Wang W, Guo W, Le L, Yu J, Wu Y, Li D, Wang Y, Wang H, Lu X, Qiao H. 2023. Integration of high-throughput phenotyping, GWAS, and predictive models reveals the genetic architecture of plant height in maize. *Molecular Plant*, **16**, 354–373.
Wang X, Zhang R, Song W, Han L, Liu X, Sun X, Luo M, Chen K, Zhang Y, Yang H. 2019. Dynamic plant height QTL revealed in maize through remote sensing phenotyping using a high-throughput unmanned aerial vehicle (UAV). *Scientific Reports*, **9**, 1–10.
Wang Z, Wang J, Peng J, Du X, Jiang M, Li Y, Han F, Du G, Yang H, Lian S. 2019a. QTL mapping for 11 agronomic traits based on a genome-wide Bin-map in a large F_2 population of foxtail millet (*Setaria italica* (L.) P. Beauv). *Molecular Breeding*, **39**, 1–13.
Wang Z, Zhang Z, Tang H, Zhang Q, Zhou G, Li X. 2019b. High-density genetic map construction and QTL mapping of leaf and needling traits in *Ziziphus jujuba* mill. *Frontiers in Plant Science*, **10**, 1424.
Watanabe K, Guo W, Arai K, Takanashi H, Kajiya-Kanegae H, Kobayashi M, Yano K, Tokunaga T, Fujiwara T, Tsutsumi N. 2017. High-throughput phenotyping of sorghum plant height using an unmanned aerial vehicle and its application to genomic prediction modeling. *Frontiers in Plant Science*, **8**, 421.
Xie J, Fernandes S B, Mayfield-Jones D, Erice G, Choi M, E Lipka A, Leakey A D. 2021. Optical topometry and machine learning to rapidly phenotype stomatal patterning traits for maize QTL mapping. *Plant Physiology*, **187**, 1462–1480.
Yan A, Ning S, Geng H, Guo T, Xiao S. 2023. Quantitative trait locus (QTL) mapping for common wheat plant heights based on unmanned aerial vehicle Images. *Agronomy*, **13**, 2088.
Yang H, Zhang Z, Zhang N, Li T, Wang J, Zhang Q, Xue J, Zhu W, Xu S. 2024. QTL mapping for plant height and ear height using bi-parental immortalized heterozygous populations in maize. *Frontiers in Plant Science*, **15**, 1371394.
Yang J, Liu Z, Chen Q, Qu Y, Tang J, Lübberstedt T, Li H. 2020. Mapping of QTL for grain yield components based on a DH population in maize. *Scientific Reports*, **10**, 7086.
Yang L, Li T, Liu B, Li R, Yu R, Zhang X, Li Q, Xu S, Xue J. 2021. Genetic analysis of ear-related traits under different pollination treatments in maize (*Zea mays*). *Plant Breeding*, **140**, 211–222.
Yang W, Feng H, Zhang X, Zhang J, Doonan J H, Batchelor W D, Xiong L, Yan J. 2020. Crop phenomics and high-throughput phenotyping: Past decades, current challenges, and future perspectives. *Molecular Plant*, **13**, 187–214.
Yang W, Guo Z, Huang C, Duan L, Chen G, Jiang N, Fang W, Feng H, Xie W, Lian X. 2014. Combining high-throughput phenotyping and genome-wide association studies to reveal natural genetic variation in rice. *Nature Communications*, **5**, 5087.
Yang W, Zhang X, Duan L. 2021. High-throughput phenotyping (HTP) and genetic analysis technologies reveal the genetic architecture of grain crops. In: Zhou J, Nguyen H T, eds., *High-Throughput Crop Phenotyping*. *Concepts and Strategies in Plant Sciences*. Springer, Cham, Switzerland. pp. 101–127.
Yu D, Zha Y, Shi L, Jin X, Hu S, Yang Q, Huang K, Zeng W. 2020. Improvement of sugarcane yield estimation by assimilating UAV-derived plant height observations. *European Journal of Agronomy*, **121**, 126159.
Yu T, Lei Y, Lu H, Zhang B, LI Y, Chen L, Ge T l, Liu Y l, Han J, LI Y. 2022. QTL analysis for plant height and fine mapping of two environmentally stable QTLs with major effects in soybean. *Journal of Integrative Agriculture*, **21**, 933–946.
Yu X, Zhang M, Yu Z, Yang D, Li J, Wu G, Li J. 2020. An SNP-based high-density genetic linkage map for tetraploid potato using specific length amplified fragment sequencing (SLAF-Seq) technology. *Agronomy*, **10**, 114.
Zhang X, Huang C, Wu D, Qiao F, Li W, Duan L, Wang K, Xiao Y, Chen G, Liu Q. 2017. High-throughput phenotyping and QTL mapping reveals the genetic architecture of maize plant growth. *Plant Physiology*, **173**, 1554–1564.
Zhou L, Gu X, Cheng S, Yang G, Shu M, Sun Q. 2020. Analysis of plant height changes of lodged maize using UAV-LiDAR data. *Agriculture*, **10**, 146.
Zhou Z, Zhang C, Lu X, Wang L, Hao Z, Li M, Zhang D, Yong H, Zhu H, Weng J. 2018. Dissecting the genetic basis underlying combining ability of plant height related traits in maize. *Frontiers in Plant Science*, **9**, 1117.
Zhou Z, Zhang C, Zhou Y, Hao Z, Wang Z, Zeng X, Di H, Li M, Zhang D, Yong H. 2016. Genetic dissection of maize plant architecture with an ultra-high density bin map based on recombinant inbred lines. *BMC Genomics*, **17**, 1–15.

Executive Editor-in-Chief Xueyong Zhang
Managing Editor Ning Wang